

Efficacy of Gold and Nickel on the Anticancer Activity and Physical Properties of Pemetrexed Loaded on Fullerene C60 Buckysomes

Ali I. A. Mahdi¹, Nidhal K. Maraie¹, Ashour H. Dawood²

¹Department of Pharmaceutics, College of Pharmacy, Mustansiriyah University, Baghdad, Iraq

²Al-Esraa University College, Baghdad, Iraq

Received: 17th August, 2022; Revised: 31st August, 2022; Accepted: 11th September, 2022; Available Online: 25th September, 2022

ABSTRACT

Objective: This study aims to create a new delivery system for pemetrexed, employing a metal-C60 fullerene combination for the first time. Additionally, a lung cancer cell line study will be used to examine the impact of this combination on the release, behavior, and drug's cytotoxicity.

Methods: To utilize a laser to irradiate hydrocarbons, fullerene C60 (Buckysomes) was produced and then nanosized by adding different volumes of isopropyl alcohol and ultrasonication. Gold Nanoparticles (AuNPs) and nickel nanoparticles (NiNPs) were also prepared each one separately and added to the previous mixture together with Pemetrexed (PMX) with further ultrasonication for 20 minutes. The mixture is kept in the refrigerator for 20 hours and then filtered. The precipitate was dried and characterized for particle size, invitro release, and anticancer activity in comparison to pemetrexed loaded on C60 fullerene previously prepared in our laboratory.

Results: The evaluation techniques revealed the successful loading of pemetrexed on metals- fullerene C60 nanocarrier, SG10 was the optimum sample with % of yield reach to 95.36. The release profile shows that the percentage release of pemetrexed after 240 minutes is equal to 40% from pure PMX, while the release after 240 minute was found to be 87.8 % from pemetrexed loaded gold nanoparticles (AuNPs) fullerene C60 nanocarrier (SG10), while NiNPs not significantly improved the release profile of Pemetrexed from Pemetrexed loaded NiNPs – fullerene (SN7). Pemetrexed loaded on gold nanoparticles (AuNPs), when compared to pure PMX (3.1 M) and SN7 (11.5 M), fullerene nanocarrier (SG10) exhibits a lower IC50 (1.55 M) and a greater cytotoxic effect (high IR percent) on A549 cancer cells. Pemetrexed's cytotoxicity in A549 was enhanced after being loaded onto gold nanoparticles (AuNPs)-fullerene nanocarriers (90.4% cell death for SG10) as opposed to pure drug (60% cell death). This finding suggests that the loading process enhanced the drug's cytotoxic activity for the tumor cells, which may have sped up the onset of action (30% cell death after 24 hours).

Conclusion: This study successfully prepared Metals- fullerene C60 Buckysomes loaded with pemetrexed utilizing gold and nickel, which may serve (especially Au- fullerene) as a suitable nanocarrier for pemetrexed, resulting in an improvement to solubility, the release pattern, and cytotoxicity.

Keywords: C60 Fullerene, Pemetrexed, Gold nanoparticles (AuNPs), Nickel nanoparticles (NiNPs), Buckysomes

International Journal of Drug Delivery Technology (2022); DOI: 10.25258/ijddt.12.3.51

How to cite this article: Mahdi, AIA, Maraie, NK, Dawood, AH, Efficacy of Gold and Nickel on the Anticancer Activity and Physical Properties of Pemetrexed Loaded on Fullerene C60 Buckysomes. International Journal of Drug Delivery Technology. 2022;12(3):1233-1244.

Source of support: Nil.

Conflict of interest: None

INTRODUCTION

In some cases, drugs with high toxic potential, such as chemotherapeutic cancer drugs, can be administered with a better safety profile using nanotechnology.¹ Nanotechnology offers multiple benefits in treating chronic human diseases through site-specific and target-oriented delivery of precise medicines. There are many types of nanocarriers, such as metal nanocarriers, quantum dots, mesoporous silica, and

carbon nanotube.² Fullerene may act as targeted and controlled drug delivery systems such as nucleic acid and viral delivery to transfer DNA, RNA, siRNA, LNA, and plasmid DNA to specific cellular locations. In some studies, nanoparticles, such as fullerenes, especially cationic ones, were used to deliver small molecules owing to their nonimmunological reactions, low cost, and high efficacy.³ Gold nanocarriers (Au NCs) have emerged as interesting tools in drug-delivery

*Author for Correspondence: Pharm.dr.nidhal.khazaal@uomustansiriyah.edu.iq

Table 1: Loading of pemetrexed and gold nanoparticles (AuNPs) on fullerene

<i>SampleNumber</i>	<i>Fullerene g</i>	<i>Isopropyl alcohol volume mL</i>	<i>Gold nanoparticles (AuNPs) g</i>	<i>Pemetrexed g</i>
SG1	0.0843	5	0.023	0.05
SG2	0.0843	10	0.023	0.05
SG3	0.0843	15	0.023	0.05
SG4	0.0843	20	0.023	0.05
SG5	0.0843	25	0.023	0.05
SG6	0.0843	30	0.023	0.05
SG7	0.0843	35	0.023	0.05
SG8	0.0843	40	0.023	0.05
SG9	0.0843	45	0.023	0.05
SG10	0.0843	50	0.023	0.05
SG11	0.0843	55	0.023	0.05
SG12	0.0843	60	0.023	0.05
SG13	0.0843	65	0.023	0.05
SG14	0.0843	70	0.023	0.05
SG15	0.0843	75	0.023	0.05

Table 2: Loading of pemetrexed and Nickel nanoparticles (NiNPs) on fullerene

<i>Sample Number</i>	<i>Fullerene g</i>	<i>Isopropyl alcohol volume mL</i>	<i>Nickel nanoparticles (NiNPs) g</i>	<i>Pemetrexed g</i>
SN1	0.0843	5	0.01436	0.05
SN2	0.0843	10	0.01436	0.05
SN3	0.0843	15	0.01436	0.05
SN4	0.0843	20	0.01436	0.05
SN5	0.0843	25	0.01436	0.05
SN6	0.0843	30	0.01436	0.05
SN7	0.0843	35	0.01436	0.05
SN8	0.0843	40	0.01436	0.05
SN9	0.0843	45	0.01436	0.05
SN10	0.0843	50	0.01436	0.05
SN11	0.0843	55	0.01436	0.05
SN12	0.0843	60	0.01436	0.05
SN13	0.0843	65	0.01436	0.05
SN14	0.0843	70	0.01436	0.05
SN15	0.0843	75	0.01436	0.05

systems due to their low toxicity, stability, easy synthesis, and reproducibility. Au NCs can link therapeutic molecules on their surface by covalent or noncovalent bonding or by a previous functionalization of Gold nanoparticle (Au NPs). They can then release the drug only in a specific site without damaging the healthy tissue.

Moreover, the small size of gold NPs allows their accumulation in sites of tumor and inflammation and exhibits fast cell uptake using mechanisms different from those typical of small molecules.⁴ Nickel (Ni) nanocarriers have been widely used in biomedical applications as antibacterial and anticancer agents. They could increase cell membrane permeability and promote cellular absorption into cancer cells of the outer target molecules.⁵ Pemetrexed is a well-known drug for the treatment

of lung cancer, but it has many serious side effects.⁶ Several trials had been reported to improve drug safety, including liposomal pemetrexed, which overcomes multi-drug resistance (MDR).^{7,8} Improve drug targeting by loading pemetrexed on chitosan nanoparticles.⁹ Another example is the loading of pemetrexed on fullerene C60 to improve anticancer activity of Pemetrexed against A549 invitro cell line study.¹⁰

The aim of this work to study the effect of introducing metals (gold/nickel) with fullerene (C60) on the loading of pemetrexed and its solubility, invitro release, and anticancer activity in order to get the optimum pemetrexed carrier that may be used to prepare an effective long-acting drug delivery system.

Table 3: Pemetrexed's percentage yield and drug loading on gold nanoparticles (AuNPs)-fullerene

<i>Formula No.</i>	<i>%Y</i>	<i>%DL</i>
SG1	76.28735	70.13
SG2	81.50	71.94
SG3	83.28	74.07
SG4	83.92	75.23
SG5	84.81	76.84
SG6	85.12	78.53
SG7	89.00	80.30
SG8	90.91	83.52
SG9	93.45	88.55
SG10	95.36	90.47
SG11	93.32	88.50
SG12	92.50	86.21
SG13	92.56	85.76
SG14	92.63	84.03
SG15	92.69	83.47

Table 4: Pemetrexed on Nickel Nanoparticles (NiNPs)-Fullerene: Yield and Drug Loading in Percentage

<i>Formula No.</i>	<i>%Y</i>	<i>%DL</i>
SN1	30.81	57.92
SN2	43.52	63.29
SN3	64.06	66.23
SN4	67.33	69.54
SN5	72.74	69.93
SN6	74.73	69.95
SN7	75.81	70.42
SN8	70.63	67.29
SN9	70.17	66.05
SN10	69.77	65.19
SN11	69.10	63.53
SN12	68.57	63.69
SN13	68.24	59.38
SN14	67.51	58.28
SN15	67.20	56.34

Table 5: Particle size and poly dispersibility index of pure pemetrexed, blank fullerene, AuNPs-fullerene, NiNPs-fullerene nanocarriers after loading with pemetrexed, blank AuNPs, and blank NiNPs.

<i>Sample</i>	<i>Particle size (Ghosh, #54)</i>	<i>Poly dispersibility index (PDI)</i>
Fullerene	232.4	0.005
Gold nanoparticles (AuNPs)- Fullerene loaded with Pemetrexed (SG10)	319.8	0.017
Nickel nanoparticles (NiNPs)- Fullerene loaded with Pemetrexed (SN7)	406.2	0.005
Blank AuNPs	27.4	0.270
Blank NiNPs	41.6	0.229

MATERIAL AND METHODS

MATERIALS

Sigma Aldrich, a company based in Germany, supplied the pemetrexed® native. The supplier of isopropyl alcohol was Himedia in India.

METHODS

Synthesis of Gold Nanoparticles (AuNPs)

The synthesis of gold nanoparticles (AuNPs) occurs by taking 1 mL of 1% chloroauric acid HAuCl_4 (10 mg/mL) added to 100 mL of deionized H_2O . After stirring to boiling, 8 mL 1% citric acid trisodium salt dihydrate $\text{Na}_3\text{C}_6\text{H}_5\text{O}_7 \cdot 2\text{H}_2\text{O}$ (10 mg/mL) was added to the boiling solution. After 15 minutes of reaction, the solution color turned reddish (the reaction was stopped). Finally, water was added to bring the volume to 100 mL and cooled to room temperature, filtered through a 0.22 μm filter, and the filtrate was stored at 4°C for 24 hours then re-filtered and the filtrate was left to dry at room temperature.¹¹

Synthesis of Nickel Nanoparticles (NiNPs)

The nickel disulfide NiS_2 nanoparticles were synthesized by taking 0.95 g Nickel chloride hexahydrate $\text{NiCl}_2 \cdot 6\text{H}_2\text{O}$ and 1.99 g Sodium thiosulfate pentahydrate $\text{Na}_2\text{S}_2\text{O}_3 \cdot 5\text{H}_2\text{O}$ dissolved in 100 mL of deionized water. The mixture solution was stirred vigorously for 10 minute.

The beaker containing the mixture solution was reacted under microwave irradiation for 10 minute. After the reaction was completed, the black precipitate was washed several times with ethanol and dried at room temperature.¹²

The prepared AuNPs and NiNPs were characterized by UV-visible spectroscopy to assess their synthesis.¹³

Loading of Fullerene with Pemetrexed and Gold Nanoparticles (AuNPs)

C60 fullerene in the amount of 80 mg was added to a 100 mL Erlenmeyer flask (previously prepared in our laboratory)¹⁰ likewise 25 mL of benzene. The mixture was ultrasonically treated for 60 minutes after being agitated for 30 min. After filtering the saturated C60 solution through filter paper, and the filtrate was allowed to cool for 30 minutes in a refrigerator. Afterward, a 100 mL vial was filled with various amounts of previously cooled iso propyl alcohol and 25 mL solution saturated with C60 fullerene, as shown in Table 1. 0.05 g of pemetrexed and 0.023 g of the produced gold nanoparticles (AuNPs) were added to the combined solution after

Table 6: Zeta potential of fullerene nanocarriers loaded with pemetrexed, blank fullerene, AuNPs-fullerene, and NiNPs-fullerene

Sample	Zeta Potential (mV)
Pemetrexed	-25.1
Fullerene	-44.8
Pemetrexed-loaded fullerene containing gold nanoparticles (AuNPs) (SG10)	-66.9
Pemetrexed-loaded nickel nanoparticles (NiNPs) on fullerene (SN7)	-32.5

20 minutes of ultrasonication, followed by another 20 minutes of ultrasonication and 20 hours in the refrigerator. The filter paper was used to separate the cold mixture, and the precipitate was then dried for three hours at 120°C in the oven.¹⁴

Loading of Fullerene with Pemetrexed and Nickel Nanoparticles (NiNPs)

80 mg of the previously synthesized C60 fullerene and 25 mL of benzene were added to a 100 mL Erlenmeyer flask. The reaction mixture was exposed to ultrasonication for 60 minutes after being agitated for 30 minutes. After filtering the saturated C60 solution through filter paper, the filtrate was allowed to cool for 30 minutes in a refrigerator. A 100 mL vial was then filled with 25 mL solution saturated with C60 Fullerene and various amounts of previously cooled isopropyl alcohol (Table 2). Following a 30 minutes ultrasonication of the combined solution, 0.05 g of pemetrexed and 0.01436 g of the produced nickel nanoparticles (NiNPs) were added. Ultrasonication continued for an additional 40 minutes, and the mixture was then chilled for 24 hours. Filter paper was used to separate the cold mixture, and the precipitate was then dried in an oven for four hours at 110°C.¹⁴

Drug Loading and Percent Yield Calculations

The weight of the resulting nanocarrier loaded with the drug was divided by the weights of fullerene, metal NPs, and the drug that was first added to the process to determine the percentage yield (percent yield),¹⁵ as follows:

$$\% \text{Yield} = \frac{\text{Weight of the obtained nanocarriers loaded with drug}}{\text{The initial weight of fullerene, drug, and metal NPs used}} * 100\%$$

The ratio of the drug in manufactured nanocarriers to the total weight of fullerene and metal NPs loaded was used to calculate the percentage of drug loading (% drug loading),¹⁶ as follow:

$$\% \text{Drug loading capacity} = \frac{\text{Weight of the drug loaded in the nanocarrier}}{\text{Total weight of fullerene and metal NPs added.}} * 100\%$$

By dissolving 10 mg of the produced drug-loaded nanocarriers in 3 mL of benzene, up to 50 mL with PBS, and read absorbance at λ_{max} 225 nm, the weight of pemetrexed loaded on distinct nanocarriers was calculated.

Selecting the Best Drug-loaded Nanocarriers

The best drug-loading nanocarrier was selected according to the best percentage of yield and drug loading capacity. They were SG10 and SN7.

Characterization of the Best Prepared Pemetrexed Loaded Nanocarriers

FTIR Measurement

For the purified Pemetrexed and PMX loaded nanocarriers SG10 and SN7, FTIR spectroscopy (4000–500 cm^{-1}) was used to characterize each one independently.¹⁷

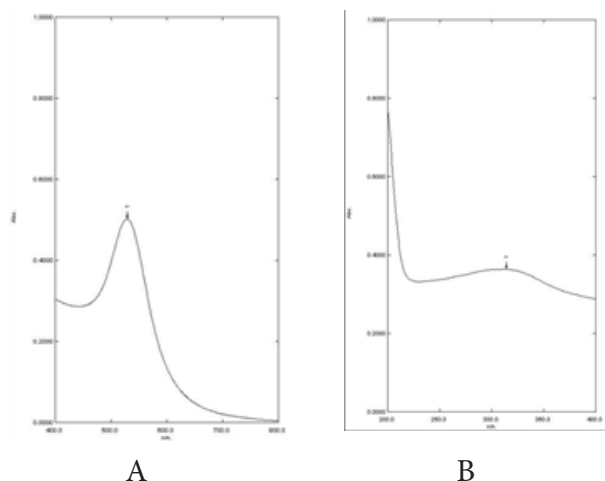


Figure 1: UV-visible spectroscopy of (A) Gold nanoparticles (AuNPs), (B) Nickel nanoparticles (NiNPs)

XRD Measurement

XRD was achieved for pure drug, drug-loaded nanocarriers SG10 and SN7 to determine their crystallinity. The XRD system was equipped with Cu-K α radiation ($\lambda = 1.54060 \text{ \AA}$), voltage (40 Kv), and current (30 mA). The samples were analyzed at a scanning speed of ($5^\circ/\text{min}$) and axis θ - 2θ with a range of 0 to 60 degrees.¹⁸

DSC Measurement

Pure drug and drug-loaded nanocarriers SG10 and SN7 underwent DSC (Differential Scanning Calorimetric) analysis by dispersing each sample (1–2 mg) in phosphate buffer (5 mL), then heating at $10^\circ\text{C}/\text{min}$ while being supplied with nitrogen gas at a rate of $10 \text{ mL}/\text{min}$.¹⁹

SEM Measurement

SEM was applied for the prepared drug-loaded nanocarriers SG10 and SN7, as well as for pure drugs. It involved taking 1-2 mg of powdered material, mounting it on a small aluminum holder, covering it with gold (a conducting metal), removing big molecules with nitrogen gas, and scanning the sample with an electron beam that was focused and fine enough to create images.²⁰

Particle Size Measurement

Dynamic light scattering is the most powerful technique for routine measurement of particle size and distribution of nanoparticle width. The native pemetrexed and best sample for drug-loaded nanocarriers SG10 and SN7 were placed in 1-cm diameter disposable cuvette to yield a suitable scattering intensity. From the analysis, the mean particle size and PDI (which is the measure of the width of size distribution) of formulas were calculated using Brookhaven Instruments Corp90 PLUS (ZetaPlus Particle Sizing, NY, Software, version 5.34). The measurements were carried out at a fixed scattering angle of 90° .^{21,22}

Measurement of the Zeta Potential

Zeta potential investigation of the drug-loaded nanocarriers SG10 and SN7, as well as pure pemetrexed, was carried out by

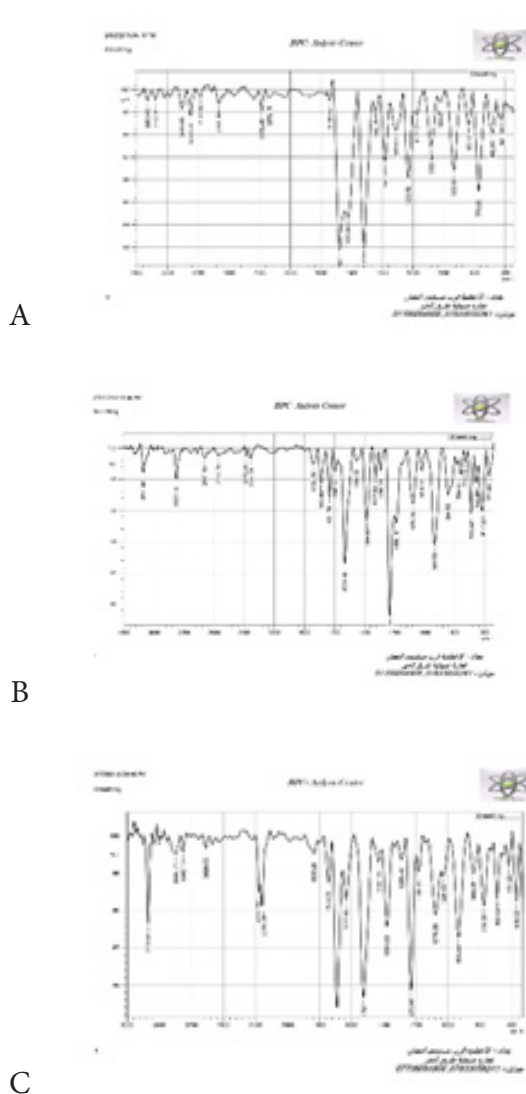


Figure 2: FTIR of (A) pure pemetrexed, (B) pemetrexed loaded on gold nanoparticles (AuNPs) – Fullerene (SG10), and (C) pemetrexed loaded on Nickel nanoparticles (NiNPs) - Fullerene (SN7)

sonicating each sample (2 mg) in PBS (10 mL) and filtering the mixture with a 0.2 L filter syringe then read the zeta potential.²³

Saturated Solubility

Separately, excess amounts of the pure drug and formulas (SG10 and SN7) were introduced to DW, then shaken until equilibrium was reached after one day. The suspension was then filtered, the first 2 mL of filtrate were discarded, and the filtrate was then used to assay the medication. The amount was regarded as the drug's equilibrium or saturation solubility.²⁴

In-vitro Drug Release Study

Using a USP type II at 37°C and 100 rpm in 500 mL of PBS, the release profile for PMX from the drug-loaded nanocarriers SG10 and SN7 was completed in comparison to pure PMX. 100 mg of pure PMX and equivalent amounts of the prepared drug-loaded nanocarriers (SG10 and SN7) were dispersed in

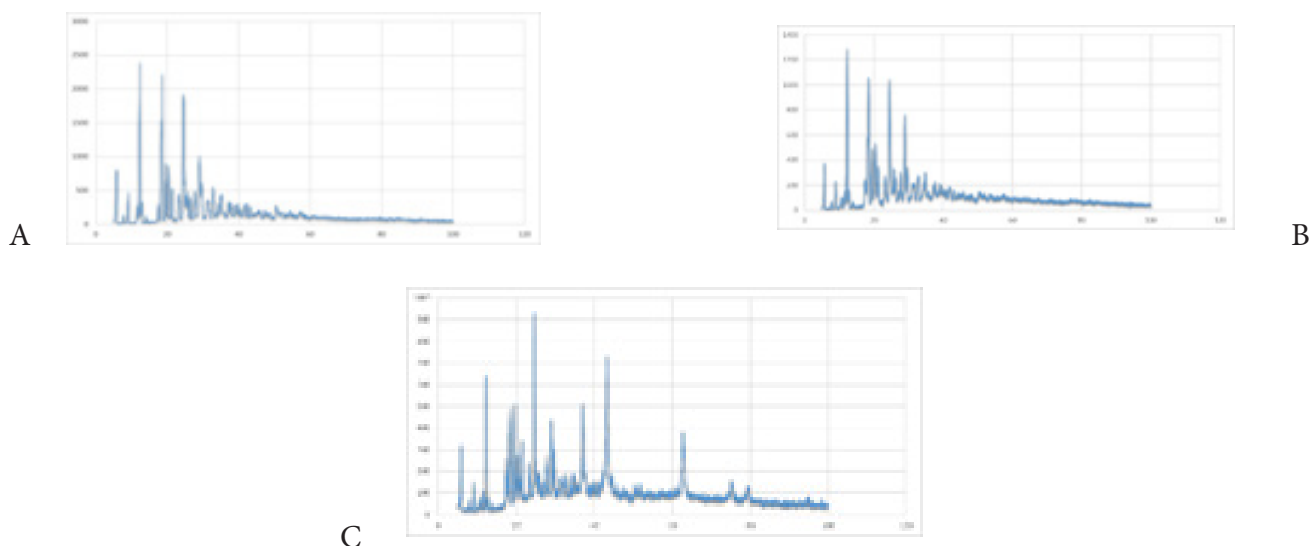


Figure 3 : XRD of (A) pure pemetrexed, (B) pemetrexed loaded on gold nanoparticles (AuNPs) – Fullerene (SG10), and (C) pemetrexed loaded on Nickel nanoparticles (NiNPs) - Fullerene (SN7)

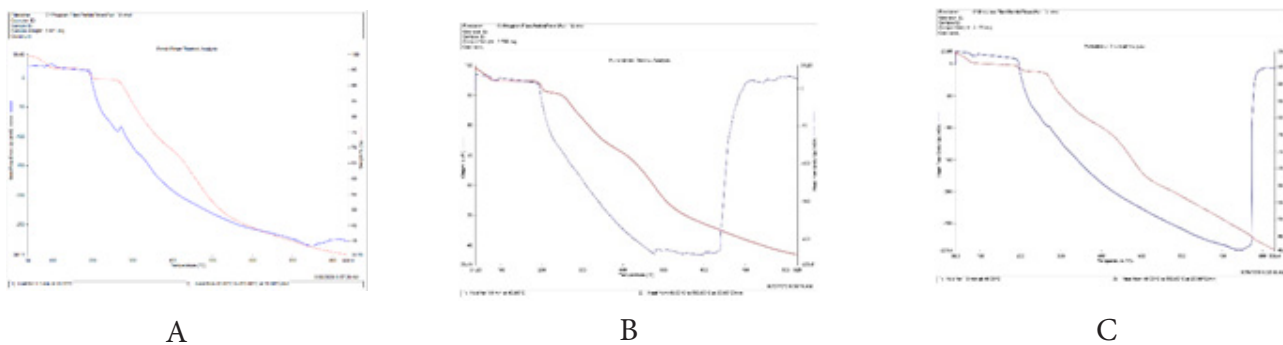


Figure 4: DSC of (A) pure pemetrexed, (B) pemetrexed loaded on gold nanoparticles (AuNPs) – Fullerene (SG10), and (C) pemetrexed loaded on Nickel nanoparticles (NiNPs) - Fullerene (SN7)

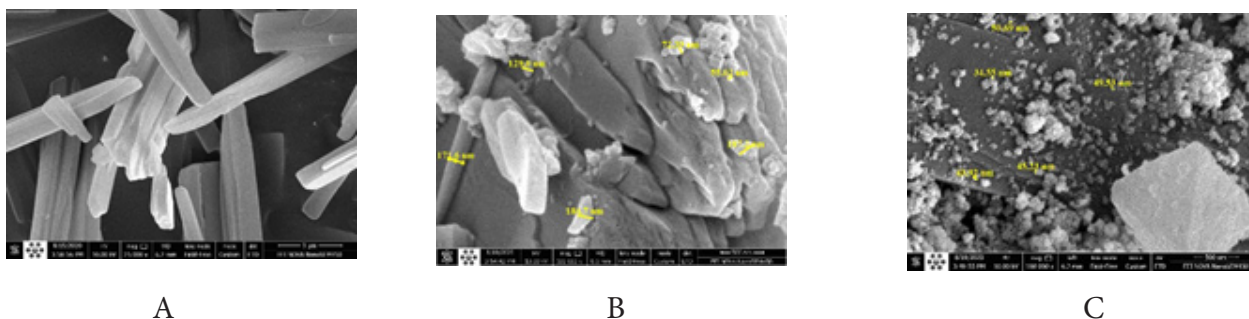


Figure 5: SEM of A) pure pemetrexed, (B) pemetrexed loaded on gold nanoparticles (AuNPs) – Fullerene (SG10), and (C) pemetrexed loaded on Nickel nanoparticles (NiNPs) - Fullerene (SN7)

the dissolution medium, and samples of 5 mL were taken out at regular intervals and replaced with the same volume of fresh media after each withdrawal. The samples were then filtered, and the content of PMX was determined spectrophotometrically by using a UV-visible spectrophotometer at 225 nm. Each experiment was examined in turn.^{25,26}

Cytotoxic activity of pemetrexed-loaded nanocarriers (SG10 and SN7)

The cytotoxic activity of pemetrexed loaded nanocarriers (SG10) and (SN7) on lung cancer cells (A549) was carried out applying the same methods, concentrations and incubation periods (24, 48 and 72 hours) applied in our previous work.^{10,27}

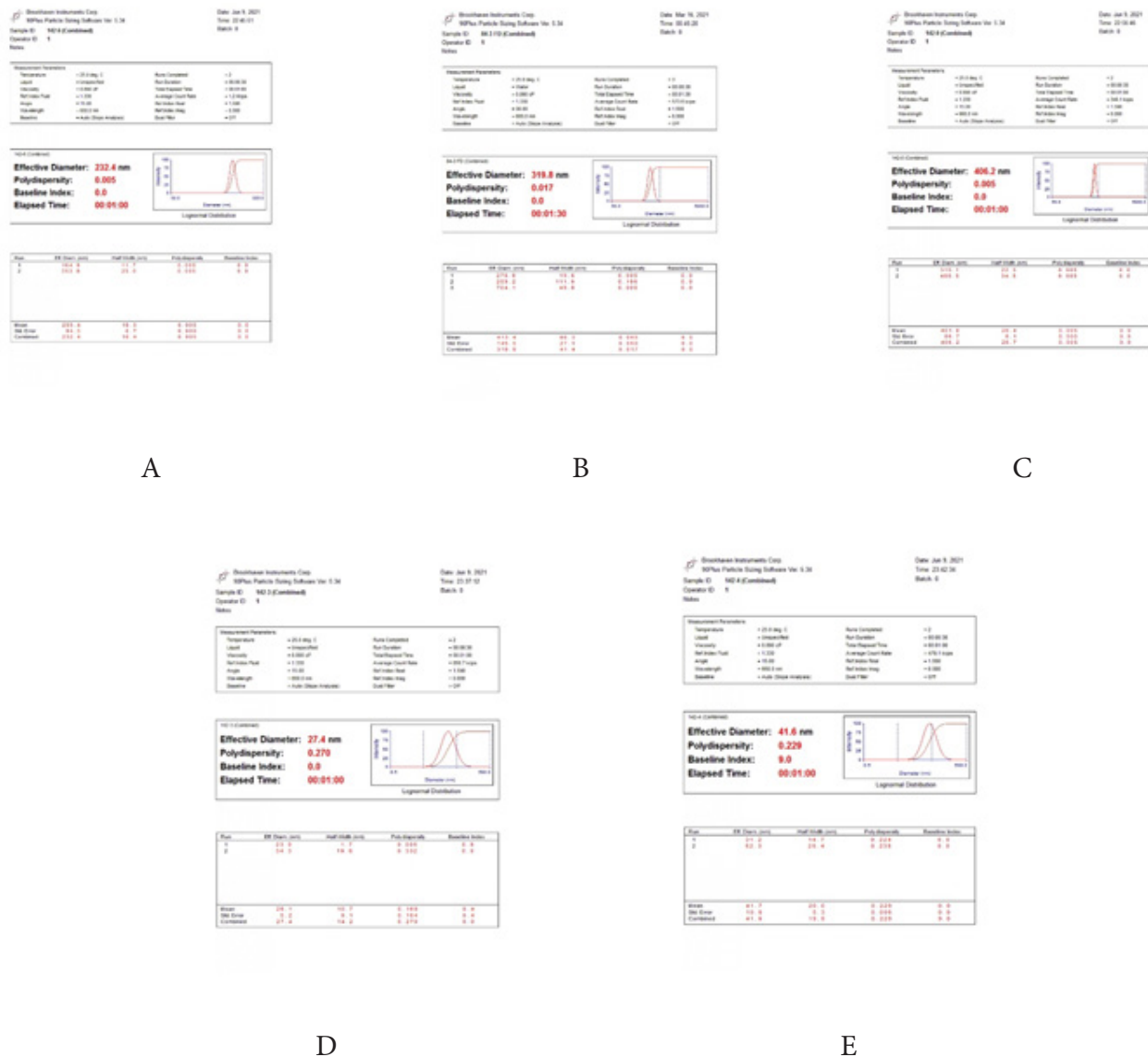


Figure 5: Particle size analysis of (A) blank fullerene and (B) pemetrexed loaded on gold nanoparticles (AuNPs) – Fullerene (SG10) (C) pemetrexed loaded on Nickel nanoparticles (NiNPs) - Fullerene (SN7) (D) blank AuNPs (E) blank NiNPs

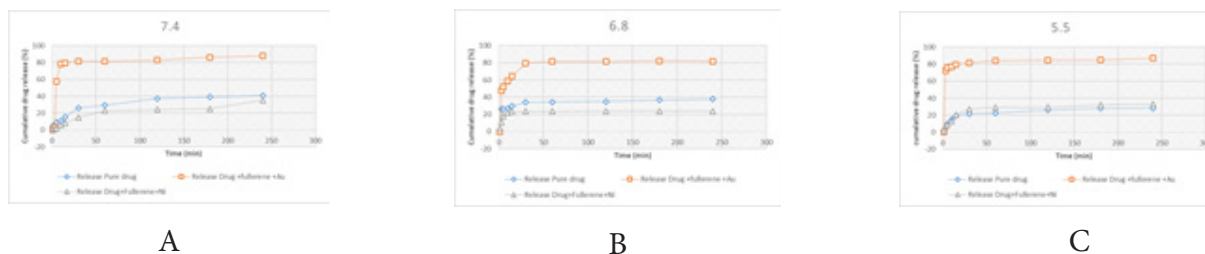


Figure 6: Comparison of the *in-vitro* release profiles of pemetrexed in its pure form and when loaded onto a metal-fullerene nanocarrier

RESULTS AND DISCUSSION

Synthesis of Gold Nanoparticles (AuNPs) and Nickel Nanoparticles (NiNPs)

Strong absorption bands were seen at 540 nm for the spectrum of AuNPs produced with citrate when the optical characteristics

of the AuNPs were studied by UV-vis absorption spectroscopy Figure 1-A, which agreed with a synthesis of gold nanoparticles through response surface modeling.²⁸ The peak position, intensity, and band shape of the Surface plasmon resonance (SPR) depend on factors such as the surrounding medium's

shape, size, composition, and dielectric constant. The citrate ions used in the work promote the reduction and stabilization of the gold nanoparticles, which leads to the mono dispersion effect.²⁹ While for Nickel nanoparticles (NiNPs), the absorption band was at 325 nm, which agreed with results observed with the preparation of nickel, nickel-iron, and silver-copper nanoparticles in ionic liquids.³⁰

Loading of Fullerene with Pemetrexed and Metal Nanoparticles

From the results in Table 3 and 4, they show that increasing the volume of isopropyl alcohol led to an increase in drug loading and percentage of yield for loading of Pemetrexed on Au- Fullerene and Ni- Fullerene, where 50 mL of isopropyl alcohol was required for loading of the drug on Au-Fullerene and gave 95.36 yields and 90.47% drug loading, while 35 mL of isopropyl alcohol was required for loading of the drug on Ni-Fullerene to give 75.8% yield and 70.42% drug loading. Above these two volumes, a non-significant ($p > 0.05$) decrease in the percentage of yield and drug loading on both carriers was observed. It is also noticed that using AuNPs gave significantly ($p < 0.05$) higher yield and drug loading than NiNPs. Isopropyl alcohol may help increase particle stabilization through its effect on Debye length and lead to blocking positive salt ions from attaching to the negatively charged surface of AuNPs, preventing aggregation and precipitation.³¹ The same result was observed with graphene oxide wrapped gold nanoparticles for intracellular Raman imaging and drug delivery.³²

For Ni-NPs, only 35 mL of isopropyl alcohol was required to stabilize its charged surface, but it gave lower yield and drug loading percentage than AuNPs due to aggregation leading to large particle size and less surface area for drug loading. The same results were observed with isopropyl alcohol to stabilize the negatively charged liposomes.³³

Therefore, the best sample that gave a higher percentage of yield and drug loading capacity on both gold and nickel NPs-fullerene carriers (SG10 and SN7) was chosen for further characterization.

Characterization of Pemetrexed loaded Nanocarriers (SG10 and SN7)

Fourier Transform Infra-Red (FTIR) Measurement

The characteristic band in the pemetrexed drug's FT-IR spectrum is at 3414 cm^{-1} ; other prominent wavelengths include

NH₂ at 3298 cm^{-1} , NH at 3170 cm^{-1} , C-H aromatic at 3050 cm^{-1} , C-H aliphatic at 2931 cm^{-1} , C=O adjacent to amide at 1743 cm^{-1} , C=O of COOH at 1698 cm^{-1} , C=N at 1624 cm^{-1} , and C=C aromatic at 1500 cm^{-1} .³⁴

The same functional groups of free pemetrexed were visible in the FT-IR spectrum of the drug-loaded on gold nanoparticles (AuNPs)-fullerene (SG10), and they are as follows: O-H of COOH is at 3417 cm^{-1} , NH₂ is at 3302 cm^{-1} , NH is at 3170 cm^{-1} , C-H aromatic is at 3030 cm^{-1} , C-H aliphatic is at 2931 cm^{-1} , C=O is next to the amide is at 1739 cm^{-1} , C=O of COOH is at 1689 cm^{-1} , C=N is at 1631 cm^{-1} , and C=C aromatic is at 1531 cm^{-1} . The same functional groups of free pemetrexed were visible in the drug's FTIR spectrum when it was loaded on nickel nanoparticles (NiNPs)-fullerene, and they were at the following wavelengths: 3394 cm^{-1} for O-H of COOH, 3302 cm^{-1} for NH₂, 3170 cm^{-1} for NH, 3020 cm^{-1} for C-H aromatic, 2931 cm^{-1} for C-H aliphatic, 1743 cm^{-1} for C=O. Both Au and Ni produced bands at 570 and 580 cm^{-1} , which are indicative of metal-drug complexes via the drug's carboxyl group. The same outcomes were seen when methotrexate was loaded onto gold and nickel nanoparticles, indicating noncovalent drug-metal nanoparticle conjugation.³⁵

Because no replaceable hydrogen atoms allow substitution processes, the conjugated pie (π) - system in fullerenes differs from that seen in classical aromatic compounds. One of two consequences is possible when a carbon atom interacts with an external chemical reagent: pie (π) bond breaking, an orbital/hybrid transition to SP₃, or a free pie (π) - orbital's contact with a chemical reagent outside the body.³⁶

The difference in Pemetrexed's FT-IR spectra before and after loading with nanocarriers indicates complicated development between pemetrexed and nanocarriers rather than a simple chemical reaction.^{37,38} The same result was observed with an anticancer drug delivery system based on carbon nanotube-dendrimer hybrid nanomaterials (Figure 2).³⁹

X-Ray Diffraction (XRD) Measurement

The free native pure Pemetrexed's XRD spectrum (Figure 3-A) shows a large number of peaks, which is evidence of its extremely stable crystalline structure. Compared to the XRD of free Pemetrexed, the XRD of Pemetrexed loaded on nanocarriers (Figure 3-B) and (Figure 3-C) reveal strong diffraction peaks with increased multiplicity but lower intensity

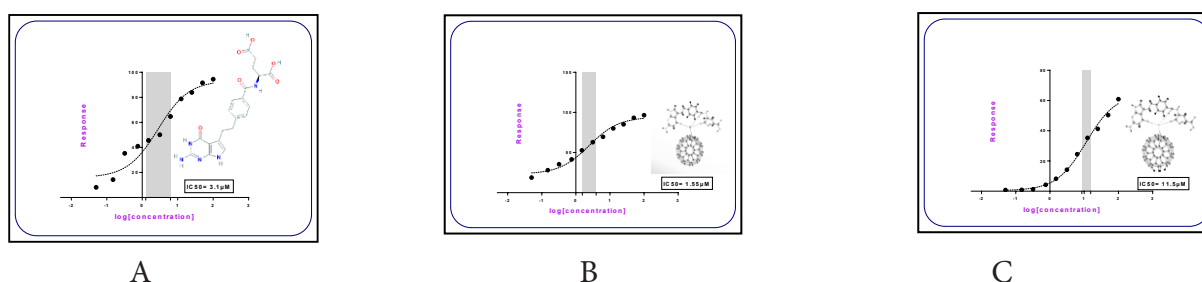


Figure 7: IC₅₀ of (A) pure pemetrexed, (B) pemetrexed loaded on gold nanoparticles (AuNPs) – Fullerene (SG10), and (C) pemetrexed loaded on Nickel nanoparticles (NiNPs) - Fullerene (SN7)

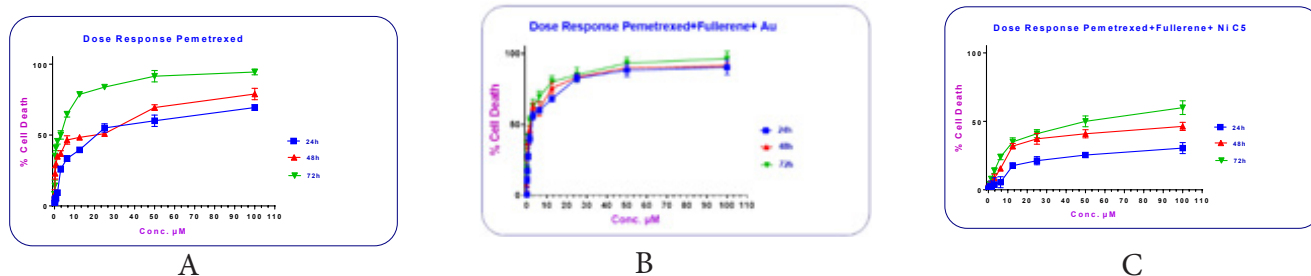


Figure 8: Dose-response curve in A549 at various concentrations (A) pure pemetrexed, (B) pemetrexed loaded on gold nanoparticles (AuNPs) – Fullerene (SG10), and (C) pemetrexed loaded on Nickel nanoparticles (NiNPs) - Fullerene (SN7) at 24, 48 and 72 hr.

and definition; however, this may be because the carriers are more amorphous.^{40,41} Fe₃O₄ nanoparticles self-assembling on carbon nanotubes produced the same outcome.⁴²

DSC Measurement

Pemetrexed's DSC spectrum (Figure 4-A) exhibits a prominent, narrow, and robust endothermic peak at 250°C, which is where the medication melts. Figure 4-B and C show a moderate, non-intense peak at 96.5°C for pemetrexed loaded on metals-fullerene nanocarriers. This points to the melting of the complex and elimination of the peak of the pemetrexed melting point.^{43,44} doxorubicin placed on multi-walled carbon nanotubes had the same results⁴⁵

SEM Measurement

The crystalline form of pure pemetrexed was visible in the photos taken under a scanning electron microscope of native pemetrexed, as illustrated in Figure 5-A.⁴⁶ Compared to the free pemetrexed, the loaded pemetrexed with nanocarriers' scanned electronic microscope (SEM) images (Figure 5-B and C) show a significantly less organized structure, showing the complex's amorphous form.⁴⁷ the same result was observed with golden single-walled carbon nanotubes prepared using double layer polysaccharides bridge for photothermal therapy⁴⁸

Particle Size Measurement

Brookhaven Instruments Corp90 PLUS was used to quantify the particle sizes of fullerene and pemetrexed loaded on nanocarriers (Figure 4 and Table 5). The particle size of fullerene was determined to be 232.4 nm, and the particle size of nanocarriers loaded with Pemetrexed SG10 and SN7 was found to be 319.8 and, 406.2 nm, respectively. The results revealed π - π bond between pemetrexed and its metal-fullerene nanocarrier that resulted in enlarging particle size. A similar result was observed upon loading pemetrexed on fullerene.¹⁰ PDI values of 0.017 and 0.005 for pemetrexed loaded on nanocarriers SG10 and SN7, respectively, suggest homogeneous distribution.⁴⁹ The same result was observed with a functionalized graphene oxide-iron oxide nanocomposite for magnetically targeted drug delivery, photothermal therapy, and magnetic resonance imaging.⁵⁰

Measurement of the Zeta Potential

The reported acceptable limit is between -30 and above, as shown in Table 6. Zeta potential values that were negative were produced by each sample used in this study (Table 6). The zeta

potential values of native pemetrexed (-25.8 mV) indicate its incipient instability, the zeta potential values of pure fullerene indicate its good stability (-44 mV), the gold nanoparticles (AuNPs)- Fullerene loaded with Pemetrexed (SG10) ZP value (-66.9) indicate it is excellent stability while nickel nanoparticles (NiNPs)- Fullerene loaded with Pemetrexed (SN7) had shown lower ZP value as compared with (SG10), and this could be attributed to the large particle size of SN7 particles.⁵¹ The same result was observed with dual targeted delivery of doxorubicin to cancer cells using folate-conjugated magnetic multi-walled carbon nanotubes.⁵²

Saturated Solubility

The solubility of pemetrexed was increased from 0.69 mg/mL (for pure drug) to 0.98 mg/mL from PMX-Au-fullerene carrier, while the reported solubility of pemetrexed loaded on fullerene was 0.72 mg/mL.¹⁰ These results indicated that introducing gold nanoparticles improved the drug solubility because the gold nanoparticles impart stability to the assembly. Also, it works on tuning surface properties such as charge and hydrophobicity.⁵⁴ The similar outcome was seen when gold nanoparticles were added to doxorubicin.⁵⁵ The results also showed that the solubility of pemetrexed from nickel-fullerene nanoparticle (SN7) was decreased to 0.61 mg/mL. This could be due to the large particle size of Nickel-fullerene loaded with PMX.⁵⁶ Similar observations were found with the DNA-Nickel complex.²⁶

In-vitro Drug Release Study

Figure 6 shows drug release from the prepared carriers SG10, and SN7 in comparison to the pure native drug in phosphate buffer pH 7.4 (physiological pH), pH 6.8 (pH of the cancer cell wall), and pH 5.5 (pH of cancer cells). The results show that the release of drug from SG10 is significantly ($p < 0.05$) higher than SN7 and pure drugs where there is a fast initial burst effect (80% within 15–20 minutes) and continued to reach 87.8% after 240 minutes while pure drug shows 30% release within 15–20 minutes and reach not more than 40% after 240 minutes. This can be attributed to the smaller particle size of SG10, high solubility, excellent stability, and high loading efficiency of the gold-fullerene nanocarrier. The same result was observed with gold nanoclusters and graphene nanocomposites for drug delivery and imaging of cancer cells.⁵⁷ The release of drug from SN7 was non-significantly ($p > 0.05$) from pure drug where low initial release that reach not more than 38.9%

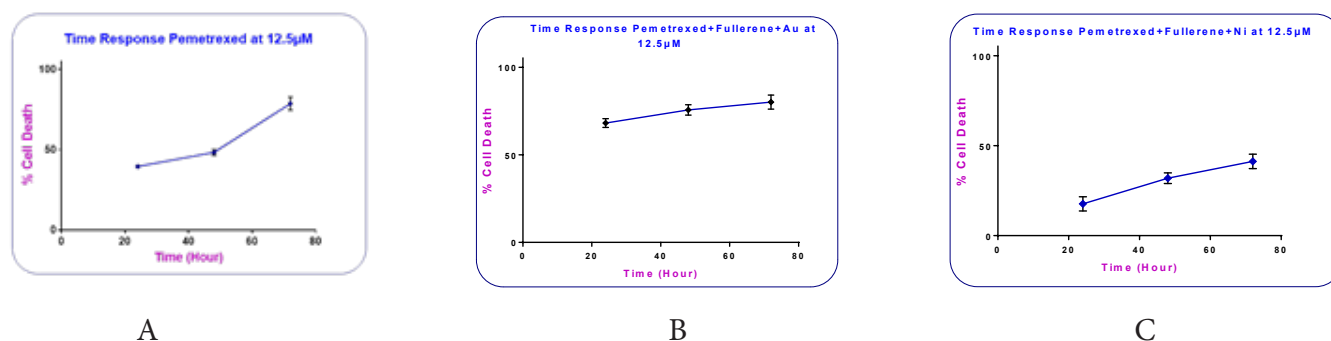


Figure 9: Time response curve in A549 at a different time of (A) (A) pure pemetrexed, (B) pemetrexed loaded on gold nanoparticles (AuNPs) – Fullerene (SG10), and (C) pemetrexed loaded on Nickel nanoparticles (NiNPs) - Fullerene (SN7)

after 240 minutes, which could be due to larger particle size (406.2 nm), low drug loading efficiency (70.42%), low solubility than gold fullerene carrier (SG10). Similar results were observed with paclitaxel loaded on nickel nanoparticles.²⁶

Cytotoxic Activity of Pemetrexed loaded Nanocarrier

Each sample was dissolved in DMSO, which has low or insignificant cytotoxic effect on both tumor and normal cells (inhibition rate percent IR percent) before and after loading with AuNPs or NiNPs -fullerene nanocarriers.⁵⁸ At different exposure times (24, 48, and 72 hours), pemetrexed loaded with gold nanoparticles (AuNPs)-fullerene nanocarrier (SG10) had a lower IC₅₀ (1.55 μM) and a higher cytotoxic effect on A549 cancer cells (Figure 7). So drug loaded on Au-fullerene had significantly lower IC₅₀ than the pure drug, which revealed the significant contribution of AuNPs available in reducing IC₅₀ of pemetrexed. The same result was observed with AuNPs with gallic acid, which improved the drug's antitumor properties for tumor cells.⁵⁹

A549 lung cancer cells were treated with pemetrexed loaded on AuNPs-fullerene (SG10) nanocarriers (Figure 8), which resulted in a higher cell death rate (90.4% cell death for SG10) than the free drug (60% cell death) after 24 hours. When pemetrexed was loaded onto nanocarriers, the cytotoxic effect was increased upon increasing its concentration throughout the time periods of 24, 48, and 72 hours. While pemetrexed loaded on Nickel nanoparticles (NiNPs) - Fullerene (SN7) resulted in a decrease percentage of cell death (30% cell death). NiNPs-fullerene loaded with pemetrexed showed lower cytotoxic activity than AuNPs-fullerene loaded with pemetrexed that could be due to decreased solubility of pemetrexed after loading with NiNPs-fullerene. The same result was observed with Targeting chemo-photothermal therapy of hepatoma by gold nanorods/graphene oxide core/shell nanocomposites.⁶⁰

Figure 9's time response curve showed that native pemetrexed concentrations of 12.5 μM at 24 hours resulted in (40% cell death), at 48 hours (45% cell death) and at 72hr (78% cell death). When compared to native pemetrexed, which shows a lower percentage of cell death (40%) at 24 hours, pemetrexed loaded on AuNPs-fullerene nanocarrier (SG10) exhibits a higher percentage of cell death (68.16%). This difference may be due to the synergistic effect of AuNPs-

fullerene on the cytotoxic effect of pemetrexed in its complex (SG10), which may result in a quicker onset of. While NiNPs led to decrease anticancer activity of pemetrexed loaded with NiNPs- Fullerene (SN7) which gave lower percentage of cell death (20% cell death at 24 hours) than that of pure pemetrexed, therefore; Pemetrexed loaded on AuNPs showed faster and high cytotoxic activity than NiNPs and pure pemetrexed that can give faster onset of action and prolong duration of action. The same result was observed with quercetin loaded with NiNPs and a Multifunctional branched gold-carbon nanotube hybrid for cell imaging and drug delivery.^{61,62}

CONCLUSION

The work revealed that introducing gold nanoparticles with fullerene significantly affected loading of pemetrexed, improved solubility, and had a fast initial burst effect in drug release and remarkably higher cytotoxic activity than NiNPs and the pure drug. Therefore, a drug-loaded on gold -fullerene complex is a good candidate for the preparation of an effective drug delivery system with a faster onset of action and long duration that may reduce the dose of drug leading to reducing its serious side effects.

ACKNOWLEDGEMENT

The authors would like to thank Mustansiriyah University (www.uomustansiriyah.edu.iq) Baghdad Iraq for its support of the present work.

CONFLICT OF INTEREST:

The authors declare no conflict of interest.

REFERENCES:

- Sahu T, Ratre YK, Chauhan S, Bhaskar LVKS, Nair MP, Verma HK. Nanotechnology based drug delivery system: Current strategies and emerging therapeutic potential for medical science. *Journal of Drug Delivery Science and Technology*. 2021;63:102487.
- Giner-Casares JJ, Henriksen-Lacey M, Coronado-Puchau M, Liz-Marzán LM. Inorganic nanoparticles for biomedicine: where materials scientists meet medical research. *Materials Today*. 2016;19(1):19-28.
- Youn YS, Kwag DS, Lee ES. Multifunctional nano-sized fullerenes for advanced tumor therapy. *Journal of Pharmaceutical*

- Investigation. 2017;47(1):1-10.
- Lacroce E, Saccomandi P, Rossi F. Can gold nanoparticles improve delivery performance of polymeric drug-delivery systems? : Future Science; 2021.
 - Jaji N-D, Lee HL, Hussin MH, Akil HM, Zakaria MR, Othman MBH. Advanced nickel nanoparticles technology: From synthesis to applications. *Nanotechnology Reviews*. 2020;9(1):1456-80.
 - Zaludek B, Van Jacobus THE. Stable and water soluble pharmaceutical compositions comprising pemetrexed. Google Patents; 2016.
 - Bai F, Yin Y, Chen T, Chen J, Ge M, Lu Y, et al. Development of liposomal Pemetrexed for enhanced therapy against multi-drug resistance mediated by ABCG5 in breast cancer. *International journal of nanomedicine*. 2018;13:1327.
 - Essam Eldin N, Elnahas HM, Mahdy MA, Ishida T. Liposomal pemetrexed: formulation, characterization and in vitro cytotoxicity studies for effective management of malignant pleural mesothelioma. *Biological & pharmaceutical bulletin*. 2015;38(3):461-9.
 - Chen J, Yang X, Huang L, Lai H, Gan C, Luo X. Development of dual-drug-loaded stealth nanocarriers for targeted and synergistic anti-lung cancer efficacy. *Drug Deliv*. 2018;25(1):1932-42.
 - Ali Imad Abdul Mahdi, Maraie N. K. , Dawood AH. Loading of Pemetrexed on synthesized fullerene C60 as a promising Buckysomes. *International Journal of Drug Delivery Technology*. 2022;12(1).
 - Hussain MH, Abu Bakar NF, Mustapa AN, Low K-F, Othman NH, Adam F. Synthesis of Various Size Gold Nanoparticles by Chemical Reduction Method with Different Solvent Polarity. *Nanoscale Research Letters*. 2020;15(1):140.
 - Kim KH, Ko WB. Preparation of C60 Nanowhiskers/NiS₂ Nanocomposites and Photocatalytic Degradation of Organic Dyes. *Asian Journal of Chemistry*. 2015;27(5):1811-4.
 - Wang B, Yang G, Chen J, Fang G. Green synthesis and characterization of gold nanoparticles using lignin nanoparticles. *Nanomaterials*. 2020;10(9):1869.
 - Ko JW, Ko WB. Synthesis of bipyramidal gold nanoparticle-[C60] fullerene nanowhisker composites and catalytic reduction of 4-nitrophenol. *Fullerenes, Nanotubes and Carbon Nanostructures*. 2017;25(12):710-5.
 - Pinto JMO, Leao AF, Alves GF, Mendes C, Franca MT, Fernandes D, et al. New supersaturating drug delivery system as strategy to improve apparent solubility of candesartan cilexetil in biorelevant medium. *Pharm Dev Technol*. 2020;25(1):89-99.
 - Long W, Ouyang H, Wan W, Yan W, Zhou C, Huang H, et al. "Two in one": Simultaneous functionalization and DOX loading for fabrication of nanodiamond-based pH responsive drug delivery system. *Mater Sci Eng C Mater Biol Appl*. 2020;108:110413.
 - Jiang L, Liu X, Xuan G. Preparation of pH-Sensitive β -Cyclodextrin Derivatives and Evaluation of Their Drug-Loading Properties. *IOP Conference Series: Materials Science and Engineering*. 2020;774.
 - Sadaquat H, Akhtar M. Comparative effects of β -cyclodextrin, HP- β -cyclodextrin and SBE7- β -cyclodextrin on the solubility and dissolution of docetaxel via inclusion complexation. *Journal of Inclusion Phenomena and Macrocyclic Chemistry*. 2020.
 - Zielinska A, Ferreira NR, Feliczak-Guzik A, Nowak I, Souto EB. Loading, release profile and accelerated stability assessment of monoterpenes-loaded solid lipid nanoparticles (SLN). *Pharm Dev Technol*. 2020:1-13.
 - Dhavale RP, Dhavale R, Sahoo S, Kollu P, Jadhav S, Patil P, et al. Chitosan coated magnetic nanoparticles as carriers of anticancer drug Telmisartan: pH-responsive controlled drug release and cytotoxicity studies. *Journal of Physics and Chemistry of Solids*. 2021;148:109749.
 - Rahman HS, Rasedee A, How CW, Abdul AB, Zeenathul NA, Othman HH, et al. Zerumbone-loaded nanostructured lipid carriers: preparation, characterization, and antileukemic effect. *International journal of nanomedicine*. 2013;8:2769.
 - Li H, Zhang N, Hao Y, Wang Y, Jia S, Zhang H, et al. Formulation of curcumin delivery with functionalized single-walled carbon nanotubes: characteristics and anticancer effects in vitro. *Drug Delivery*. 2014;21(5):379-87.
 - Zugic A, Tadic V, Savic S. Nano- and Microcarriers as Drug Delivery Systems for Usnic Acid: Review of Literature. *Pharmaceutics*. 2020;12(2).
 - Stewart AM, Grass ME. Practical approach to modeling the impact of amorphous drug nanoparticles on the oral absorption of poorly soluble drugs. *Molecular pharmaceutics*. 2019;17(1):180-9.
 - Pande VV, Khedkar PV, Giri MA, Pote AK, Polshettiwar SA. Fabrication and Characterisation of gemcitabine hydrochloride loaded magnetically responsive mesoporous silica nanocomposites as smart hybrid theranostic platform for treatment of pancreatic cancer. *Materials Technology*. 2020:1-8.
 - Abdulbaqi MR, Maraie N. K., Dawood AH. Loading of clarithromycin and paclitaxel on synthesized CDS/NIO nanoparticles as promising nanocarriers. *Int J Pharm Pharm Sci*. 2016;8(5):322-33.
 - Jasim B. Redounding of *Cuscuta chinensis* Lam. on BxPC-3, HepG2, and U2OS Human Cancer Cell Lines. *International Journal of Drug Delivery Technology*. 2020;10:354-9.
 - Oliveira JP, Prado AR, Keijok WJ, Ribeiro MRN, Pontes MJ, Nogueira BV, et al. A helpful method for controlled synthesis of monodisperse gold nanoparticles through response surface modeling. *Arabian Journal of Chemistry*. 2020;13(1):216-26.
 - Martínez J, Chequer N, González J, Cordova T. Alternative methodology for gold nanoparticles diameter characterization using PCA technique and UV-VIS spectrophotometry. *Nanosci Nanotechnol*. 2012;2(6):184-9.
 - Lobotka P, Radnóczy G, Czigany Z, Vavra I, Drzik M, Micusik M, et al., editors. Preparation of nickel, nickel-iron, and silver-copper nanoparticles in ionic liquids. 2013 *Transducers & Eurosensors XXVII: The 17th International Conference on Solid-State Sensors, Actuators and Microsystems (TRANSDUCERS & EUROSENSORS XXVII)*; 2013: IEEE.
 - Ma X, Qu Q, Zhao Y, Luo Z, Zhao Y, Ng KW, et al. Graphene oxide wrapped gold nanoparticles for intracellular Raman imaging and drug delivery. *Journal of Materials Chemistry B*. 2013;1(47):6495-500.
 - Liu Z, Lanier OL, Chauhan A. Poly (Vinyl Alcohol) Assisted Synthesis and Anti-Solvent Precipitation of Gold Nanoparticles. *Nanomaterials*. 2020;10(12):2359.
 - Webb C, Khadke S, Schmidt ST, Roces CB, Forbes N, Berrie G, et al. The Impact of Solvent Selection: Strategies to Guide the Manufacturing of Liposomes Using Microfluidics. *Pharmaceutics*. 2019;11(12):653.
 - Vandana M, Sahoo SK. Reduced folate carrier independent internalization of PEGylated pemetrexed: a potential nanomedicinal approach for breast cancer therapy. *Mol Pharm*. 2012;9(10):2828-43.

35. Chen YH, Tsai CY, Huang PY, Chang MY, Cheng PC, Chou CH, et al. methotrexate conjugated to gold nanoparticles inhibits tumor growth in a syngeneic lung tumor model. *Mol Pharm.* 2007;4(5):713-22.
36. Park S, Srivastava D, Cho K. Endo-fullerene and doped diamond nanocrystallite-based models of qubits for solid-state quantum computers. *Journal of nanoscience and nanotechnology.* 2001;1(1):75-81.
37. Frazao NF, Albuquerque EL, Fulco UL, Azevedo DL, Mendonça GL, Lima-Neto P, et al. Four-level levodopa adsorption on C 60 fullerene for transdermal and oral administration: a computational study. *RSC advances.* 2012;2(22):8306-22.
38. Hamed TM, Dawood AH, Arif IS, Saihood YD. In Vivo Study of the Anticancer Activity of Doxorubicin Loaded on a Cellulose-Based Nanocarrier System. *Al-Mustansiriyah Journal of Pharmaceutical Sciences (AJPS).* 2018;18(2):33-40.
39. Mehdipoor E, Adeli M, Bavadi M, Sasanpour P, Rashidian B. A possible anticancer drug delivery system based on carbon nanotube–dendrimer hybrid nanomaterials. *Journal of Materials Chemistry.* 2011;21(39):15456-63.
40. Veisi H, Masti R, Kordestani D, Safaei M, Sahin O. Functionalization of fullerene (C60) with metformine to immobilized palladium as a novel heterogeneous and reusable nanocatalyst in the Suzuki–Miyaura coupling reaction at room temperature. *Journal of Molecular Catalysis A: Chemical.* 2014;385:61-7.
41. Kadhium HS, Maraie NK. Preparation and in Vitro Evaluation of Soya Lecithin Based Nano Transfersomal Dispersion for Loxoprofen Sodium. *Al-Mustansiriyah Journal of Pharmaceutical Sciences (AJPS).* 2019;19(4):102-15.
42. Liu Y, Jiang W, Li S, Li F. Electrostatic self-assembly of Fe₃O₄ nanoparticles on carbon nanotubes. *Applied Surface Science.* 2009;255(18):7999-8002.
43. Küçüktürkmen B, Bozkır A. Development and characterization of cationic solid lipid nanoparticles for co-delivery of pemetrexed and miR-21 antisense oligonucleotide to glioblastoma cells. *Drug development and industrial pharmacy.* 2018;44(2):306-15.
44. Luo J, Lin M, Zhu Z, Luo J, Ye W, Qin Y, et al. Crystalline forms of Pemetrexed diacid, and preparations thereof. *Google Patents;* 2012.
45. Uttekar PS, Lakade SH, Beldar VK, Harde MT. Facile synthesis of multi-walled carbon nanotube via folic acid grafted nanoparticle for precise delivery of doxorubicin. *IET nanobiotechnology.* 2019;13(7):688-96.
46. Soni K, Mujtaba A, Akhter MH, Kohli K. The Development of Pemetrexed Diacid-Loaded Gelatin-Cloisite 30B (MMT) Nanocomposite for Improved Oral Efficacy Against Cancer: Characterization, In-Vitro and Ex-Vivo Assessment. *Current drug delivery.* 2020;17(3):246-56.
47. Majeed S, Maraie N. K. , Ashour D. Preparation and Comparative Evaluation of Fe²⁺/Fe³⁺ and Mg²⁺/Fe³⁺ LDHs as Promising Nanocarriers for Class II and Class IV Drugs. 2015.
48. Meng L, Xia W, Liu L, Niu L, Lu Q. Golden Single-Walled Carbon Nanotubes Prepared Using Double Layer Polysaccharides Bridge for Photothermal Therapy. *ACS Applied Materials & Interfaces.* 2014;6(7):4989-96.
49. Khan I, Khan I, Usman M, Imran M, Saeed K. Nanoclay-mediated photocatalytic activity enhancement of copper oxide nanoparticles for enhanced methyl orange photodegradation. *Journal of Materials Science: Materials in Electronics.* 2020;31(11):8971-85.
50. Ma X, Tao H, Yang K, Feng L, Cheng L, Shi X, et al. A functionalized graphene oxide-iron oxide nanocomposite for magnetically targeted drug delivery, photothermal therapy, and magnetic resonance imaging. *Nano Research.* 2012;5(3):199-212.
51. Unterweger H, Tietze R, Janko C, Zaloga J, Lyer S, Dürr S, et al. Development and characterization of magnetic iron oxide nanoparticles with a cisplatin-bearing polymer coating for targeted drug delivery. *International journal of nanomedicine.* 2014;9:3659.
52. Lu Y-J, Wei K-C, Ma C-CM, Yang S-Y, Chen J-P. Dual targeted delivery of doxorubicin to cancer cells using folate-conjugated magnetic multi-walled carbon nanotubes. *Colloids and Surfaces B: Biointerfaces.* 2012;89:1-9.
53. Kumar A, Dixit CK. 3 - Methods for characterization of nanoparticles. In: Nimesh S, Chandra R, Gupta N, editors. *Advances in Nanomedicine for the Delivery of Therapeutic Nucleic Acids:* Woodhead Publishing; 2017. p. 43-58.
54. Ghosh P, Han G, De M, Kim CK, Rotello VM. Gold nanoparticles in delivery applications. *Advanced Drug Delivery Reviews.* 2008;60(11):1307-15.
55. Aryal S, Grailler JJ, Pilla S, Steeber DA, Gong S. Doxorubicin conjugated gold nanoparticles as water-soluble and pH-responsive anticancer drug nanocarriers. *Journal of Materials Chemistry.* 2009;19(42).
56. Xiao Y-N, Zhang C-X. The interaction of DNA and water-soluble polymeric Schiff-base nickel complexes. *Bulletin of the Chemical Society of Japan.* 2002;75(7):1605-9.
57. Wang C, Li J, Amatore C, Chen Y, Jiang H, Wang XM. Gold nanoclusters and graphene nanocomposites for drug delivery and imaging of cancer cells. *Angew Chem Int Ed Engl.* 2011;50(49):11644-8.
58. Aslan HG, Akkoç S, Kökbudak Z. Anticancer activities of various new metal complexes prepared from a Schiff base on A549 cell line. *Inorganic Chemistry Communications.* 2020;111:107645.
59. Rattanata N, Daduang S, Wongwattanakul M, Leelayuwat C, Limpaboon T, Lekphrom R, et al. Gold Nanoparticles Enhance the Anticancer Activity of Gallic Acid against Cholangiocarcinoma Cell Lines. *Asian Pacific journal of cancer prevention : APJCP.* 2015;16(16):7143-7.
60. Xu C, Yang D, Mei L, Li Q, Zhu H, Wang T. Targeting chemophotothermal therapy of hepatoma by gold nanorods/graphene oxide core/shell nanocomposites. *ACS Appl Mater Interfaces.* 2013;5(24):12911-20.
61. Rameshthangam P, Chitra JP. Synergistic anticancer effect of green synthesized nickel nanoparticles and quercetin extracted from *Ocimum sanctum* leaf extract. *Journal of Materials Science & Technology.* 2018;34(3):508-22.
62. Minati L, Antonini V, Dalla Serra M, Speranza G. Multifunctional Branched Gold–Carbon Nanotube Hybrid for Cell Imaging and Drug Delivery. *Langmuir.* 2012;28(45):15900-6.